Dynamic model of a flexible blade wind turbine in an electrical grid control structure

Lamine Chalal, Jean-Yves Dieulot, Geneviève Dauphin-Tanguy, Frédéric Colas

DYNAMIC MODEL OF A FLEXIBLE BLADE WIND TURBINE IN AN ELECTRICAL GRID CONTROL STRUCTURE

Lamine CHALAL [(a)], Jean Yves DIEULOT[(b)], Genevieve DAUPHIN-TANGUY[(a)] , Frederic COLAS[(c)]

[(a)] LAGIS FRE CNRS 3303, Ecole Centrale de Lille, BP 48, 59651 Villeneuve d'Ascq Cedex, France
[(b)] LAGIS FRE CNRS 3303, Polytech'Lille, Cité Scientifique, 59655 Villeneuve d'Ascq Cedex, France
[(c)] L2EP, ENSAM, 8 Bd Louis XIV, 59000 Lille

[(a)]laminechalal@gmail.com, [(b)]jean-yves.dieulot@polytech-lille.fr , [(c)]genevieve.dauphin-tanguy@ec-lille.fr, [(d)]Frederic.COLAS@ensam.eu

ABSTRACT
It has already been reported that one-mass or lumped model of wind turbine system is insufficient to analyze the transient behaviour of wind turbine. For the sake of exact analysis of transient stability of wind turbines, it is needed to consider two-mass shaft system model. This model of drive train doesn't take into account the flexibility of blades. But it is usually used to calculate the electromagnetic torque reference allowing a Maximum Power Point Tracking (MPPT) strategy at low wind speed. In this paper we will compare the behavior of the controlled system, when the blades are supposed to be rigid and when their flexibility is taken into account using the Blade Element Momentum theory (BEM).

Keywords: Wind turbine, Blade element momentum theory, flexible mechanical systems.

1. INTRODUCTION

Electrical energy generation using wind power has recently received considerable interest and attention all over the world due to growing environmental concern.

In most cases, wind turbines are modeled as a one mass lumped model having combined constant inertia.

As the one-mass lumped model is too simple for representing the dynamics of a wind turbine and wind generator connected to each other through a shaft, stability analysis based on the one-mass shaft model may give significant errors (Muyeen, Hasan Ali, Takahashi,Murata,Tamura,Tomaki, Sakahara and Sasano 2007).

The size of commercial wind turbines has increased dramatically in the last 25 years from approximately a rated power of 50kW and a rotor diameter of 10–15m up to today's commercially available 5MW machines with a rotor diameter of more than 120 m. Since the stiffness is not increasing proportionally, structures of that magnitude are severely dynamical sensitive.

Moreover, very large displacements of the blades may occur, for which reason non-linear effects cannot be ignored (Hansen, Sørensen, Voutsinas and Sørensen 2006).

Usually only the drive-train shaft flexibility is considered, but such other issues should be addressed such as the inherent flexibility of blades and tower while modeling a wind turbine system. While the latter phenomenon is well identified, wind turbines with flexible blades are reported in fewer studies (see Agarwal, Dauphin-Tanguy, and Guillaud, 2009). For wind turbine generation system, control laws are usually designed from steady state equations. The objective of this paper is to point out the consequences of such strategy in the transient phases due to the flexible modes of the blades. It will be shown the overrating and the underrating of the aerodynamic power which can be extracted from the wind turbine.

This paper is organized as followed. After the introduction, section 2 presents the procedure for determining the reference electromagnetic torque used in the control structure. The dynamic model of the wind turbine blade is presented in section 3. In section 4 we present some simulations results. Concluding remarks are given in section 4.

2. CONTROL LOOP AT LOW WIND SPEED:

The aerodynamic efficiency is the ratio of turbine power to wind power and is known as the turbine's power coefficient, C_p. C_p can be computed as:

$$C_p = \frac{P}{P_{wind}} \cdot \quad (1)$$

where P is the power captured by the turbine and P_{wind} is the power available in the wind for a turbine of that size. The power P_{wind} is given by:

$$P_{wind} = \frac{1}{2}\rho S v^3 . \quad (2)$$

where ρ is the air density, S is the rotor swept area, and v is the wind speed.

Variable-speed wind turbines have three main operating regions. The first one, region 1, consists of the turbine startup routine. Region 2 is an operating mode during which it is desirable that the turbine captures as much power as possible from the wind.

Region 3 is encountered when the wind speed is high enough for the power to be held constant by the use of wind turbine controls. The turbine rotational speed is maintained at the desired rotational speed through the use of blade pitch angle. Figure 1 shows the overall control system in region 2 and region 3. The grid control system is not shown in the figure.

In this paper, we focus on region 2 operation, which accounts for more than 50% of yearly energy capture for a typical modern turbine (Johnson, Fingersh, Balas and Pao 2004).

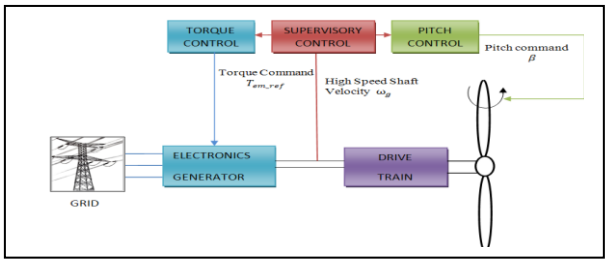

Figure1: Basic turbine control

In region 2, the wind speed and the generator torque are below "rated". Blade pitch is held constant at the optimal value that gives maximum aerodynamic torque. Each wind speed has a corresponding rotor speed at which the greatest possible aerodynamic torque is generated. It turns out that when the blade pitch is held at the optimal β_{opt}, there is a constant value tip-speed ratio λ, that maximizes aerodynamic torque . The tip-speed ratio λ, is defined as :

$$\lambda = \frac{\omega_t R_t}{v} \ . \qquad (3)$$

where ω_t is the wind turbine rotor-speed, R_t is the wind turbine rotor radius, and v is the wind velocity.

So, the control objective in Region 2 is to command electromagnetic torque so that the rotor speed ω_t tracks the wind speed v and gives an optimal tip-speed ratio λ_{opt}.

For modern HAWTs (Horizontal-Axis Wind Turbine), the relationship between the power coefficient C_p and the tip-speed ratio λ is a turbine-specific nonlinear function. C_p also depends on the blade pitch angle in a nonlinear fashion, and these relationships have the same basic shape for most modern HAWTs (Pao and Johnson 2009). So the turbine is considered as an aerodynamic torque generator.

In this work, we will use a two-mass model of the drive train. This is motivated by the fact that one mass-model cannot report the flexibility of the low speed shaft (Boukhezzar and Siguerdidjane 2009).

The masses used in the model correspond to a large turbine rotor inertia J_r, and a small inertia J_g representing the induction generator shaft (figure 2). The dynamic nature of the shaft is illustrated by damping b_{ls} and the spring K_{ls} . The gear ratio G is illustrated by the discs in the middle. Friction coefficients for the turbine and generator are represented by b_r and b_g respectively.

The equations which govern the model are given by:

$$\begin{cases} J_r\dot{\omega}_t = T_a - T_{ls} - b_r\omega_t \ . & (4) \\ \dot{\theta}_{K\_ls} = \omega_t - \omega_{ls} \ . & (5) \\ J_g\dot{\omega}_g = T_{hs} - T_{em} - b_g\omega_g \ . & (6) \end{cases}$$

with:

$T_{ls} = K_{ls}(\theta_t - \theta_{ls}) + b_{ls}(\omega_t - \omega_{ls}),\ T_{hs} = \frac{T_{ls}}{G}$ and $\omega_{ls} = \frac{\omega_g}{G}$

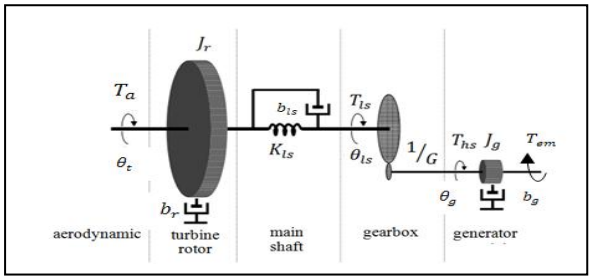

Figure 2: Two-mass Wind Turbine Scheme

In steady state, the previous set of equations becomes:

$$\begin{cases} 0 = T_a - T_{ls} - b_r\omega_t. & (7) \\ 0 = \omega_t - \omega_{ls} \ . & (8) \\ 0 = T_{hs} - T_{em} - b_g\omega_g \ . & (9) \end{cases}$$

From equation (8), we can deduce that:

$$\omega_t = \omega_{ls} = \frac{\omega_g}{G}. \qquad (10)$$

Multiplying (9) by G, and summing with (7) we obtain:

$$T_a - T_{ls} - b_r\omega_t + G\,T_{hs} - GT_{em} - Gb_g\omega_g = 0. \qquad (11)$$

After some rearranging, the electromagnetic torque is given by:

$$T_{em} = \frac{T_a}{G} - \left(b_g + \frac{b_r}{G^2}\right)\omega_g \ . \qquad (12)$$

For determining the optimal electromagnetic torque T_{em_ref} from equation (12), it is usually assumed that:

$$T_a = K_{opt}\,\omega_t^2 \ . \qquad (13)$$

where K_{opt} is derived from equations (1),(2) and (3) as:

$$K_{opt} = \frac{1}{2}\rho\pi R_t^5\ \frac{C_{p\_max}}{\lambda_{opt}^3}$$

The reference electromagnetic torque is obtained by replacing equation (13) in (12),which gives:

$$T_{em\_ref} = K_{opt\_hs}\,\omega_g^2 - K_{t\_hs}\omega_g \ . \qquad (14)$$

where:

$K_{opt\_hs} = \frac{K_{opt}}{G^3}$ and $K_{t\_hs} = b_g + \frac{b_r}{G^2}$

Equation (14) requires the knowledge of K_{opt_hs} and K_{t_hs} , which may be supplied by the turbine manufacturer.

It is reasonable to assume that the generator with a good current control system responds rapidly and accurately when tracking the reference torque produced by the torque controller.

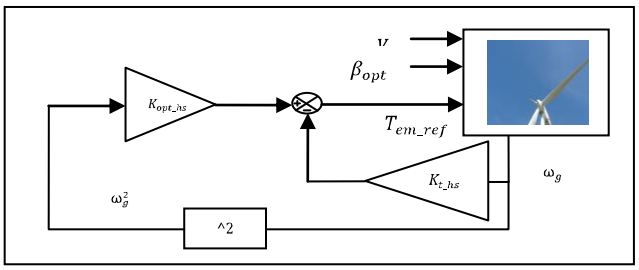

Figure 3 Generation of T_{em_ref}

3. DYNAMIC MODEL OF A WIND TURBINE BLADE:

In this paper structural model of wind turbine blade is based on Rayleigh beam model **(**Mukherjee , Karmakar, and Samantaray 2000**)**. The blade can be assumed as a twisted beam composed of a number of sections (Figure 4) submitted to aerodynamic forces calculated using the blade element momentum (BEM) theory (Agarwal, Dauphin-Tanguy, and Guillaud 2009).

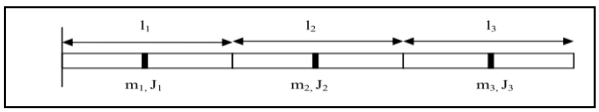

Figure 4: Blade considered as a beam (3 sections)

The forces exerted on an element of the beam are: elastic forces, damping forces, inertial forces and external forces. The bond graph model of each section can be built (figure 5):

- The stiffness matrix is modeled as a 4 – port C – field storage
- The structural damping matrix is modeled as R-field
- The inertia effects are modeled as I element

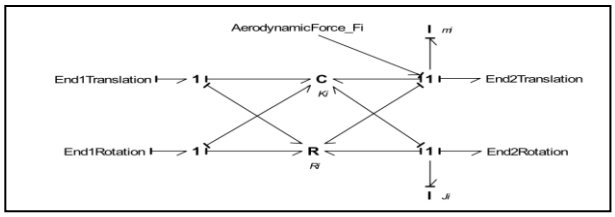

Figure 5: bond graph model of a section of the turbine blade with aerodynamic force

The mathematical model most frequently used by scientific and industrial communities is based on the blade element momentum (BEM) theory (Lanzafame and Messina 2007). Blade element theory assumes that each blade can be divided into a number of radial blade elements, where local aerodynamic loads can be calculated independently, reducing it into a 2D-problem. Then these loads are integrated in order to determine the total aerodynamic load on each blade (Pournaras, Riziotis and Kladas 2008).

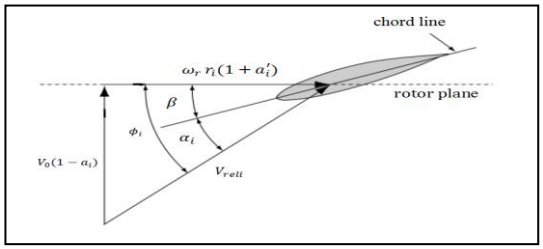

Figure 6: Local element velocities and flow angles

The relationships between the lift and drag forces and the normal and tangential forces are purely vectorial as determined by the angle of attack of the incoming flow stream α_i, defined as the angle between the incoming flow stream and the chord line of the airfoil at the i^{th} section, as shown Figure 6.

The inflow angle is for section *i* obtained from Figure 6 as:

$$\phi_i = tan^{-1}\left(\frac{V_0(1-a_i)}{\Omega_{ri}(1+a_i')}\right) . \qquad (15)$$

Figure 7 shows the resultant aerodynamic forces on the element and their components perpendicular and parallel to the rotor plane. The dF_n is normal to the plane of rotation (contributing to thrust force) while dF_t is the force tangential to the rotor plane creating the useful torque. The aforementioned forces are the dominating ones in turbine design(Moriarty and Hansen 2007).

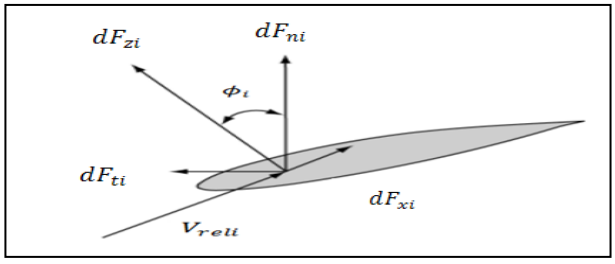

Figure 7: Local forces on a blade

The aerodynamic forces (dF_{zi} and dF_{xi}), per blade unit length, are calculated by means of the corresponding aerodynamic coefficients C_{zi} (lift coefficient) and C_{xi} (drag coefficient) which are known for each blade element , as follows:

$$dF_{zi} = \frac{1}{2}\rho c_i C_{zi} {V_{rel}}^2 . \qquad (16)$$

$$dF_{xi} = \frac{1}{2}\rho c_i C_{xi} {V_{rel}}^2 . \qquad (17)$$

where ρ is the air density ,c_i the chord of each blade element and V_{rel} is the relative velocity. The lift (C_{zi}) and drag (C_{xi})coefficient are calculated by using

look-up tables which are functions of the angle of attack α_i.

The local force components for each blade element, per unit length, as shown in Figure 7 are calculated normal to and tangential to the rotor plane as follows:

$$dF_{ni} = dF_{zi}\cos\phi_i + dF_{xi}\sin\phi_i. \quad (18)$$
$$dF_{ti} = dF_{zi}\sin\phi_i - dF_{xi}\cos\phi_i. \quad (19)$$

One of the major limitations of the original BEM theory is that there is no influence of vortices shed from the blade tips into the wake on the induced velocity field. This tip vortex creates multiple helical structures in the wake, and they play a major role in the induced velocity distribution at the rotor, so a correction factor F_i, named Prandtl tip-loss factor, is introduced for the calculation of the corrected induction factors a_i and a_i' and is computed as follows :

$$F_i = \frac{2}{\pi} cos^{-1}\left(e^{\left[\frac{-B(R_t - r_i)}{2\, r_i \sin\phi_i}\right]}\right). \quad (20)$$

where B is the number of blades, R_t is the overall radius of rotor and r_i is the local radius of blade element.

The corrected values for the induction factors a_i and a_i', are given by the following equation (Moriarty and Hansen 2007) :

$$a_i = \frac{1}{\frac{4F_i \sin\phi_i{}^2}{\sigma_i C_{ni}} + 1}. \quad (21)$$

$$a_i' = \frac{1}{\frac{4F_i \sin\phi_i \cos\phi_i}{\sigma_i C_{ti}} - 1}. \quad (22)$$

where

- $\sigma_i = \frac{Bc_i}{2\pi r_i}$
- $C_{ni} = C_{zi}\cos\phi_i + C_{xi}\sin\phi_i$
- $C_{ti} = C_{zi}\sin\phi_i - C_{xi}\cos\phi_i$

The aerodynamic force F_{a_i} exerted on each blade section, is calculated using the following equation:

$$F_{a\_i} = \left(\frac{1}{2}\rho V_0 \frac{(1-a_i)^2}{\sin\phi_i{}^2}(C_{zi}\sin\phi_i - C_{xi}\cos\phi_i)c_i\, l_i\right)V_0 . \quad (23)$$

Now that all of the equations for BEM theory have been established, the iteration procedure used to calculate the exerted force F_{a_i} on each section is implemented in gyrator element GY_i (Agarwal, Dauphin-Tanguy, and Guillaud 2009).

Figure 8 shows a bond graph model of the blade (three sections), where:

- Sf: V_0 represents the wind mean velocity
- Sf: represents the angular velocity of the rotor ω_t.
- Sf: *Vbound* and Se define the boundary conditions.
- Gyrators have two input modulating signals; one is the pitch of the blade β, which is a control variable, and the other is the angular velocity of the rotor ω_t.
- J_{whole} is the rigid body inertia of the whole blade.

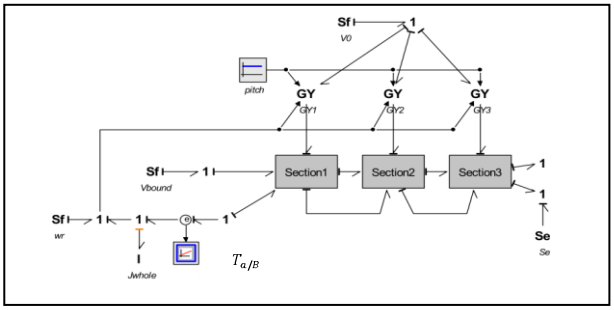

Figure 8 : Bond graph Model of turbine blade (three sections)

The resultant aerodynamic torque T_a is calculated by multiplying the aerodynamic torque, obtained from the bond graph model of single blade, by the number of blades B.

4. SIMULATION RESULTS

The numerical simulations were performed on a wind turbine whose characteristics are given in Table I.

For simulating the controlled wind turbine system, we will use two different models of the wind turbine as shown in figure 8, the first one including a dynamic model of flexible blades, the second one corresponding to an algebraic model of blades supposed rigid. The bond graph model of flexible blades (Figure 8) is connected to the two mass model described in section 2.

The inertia of each blade, which is represented by J_{whole} in figure 8, is lumped with the other wind turbine components: hub inertia and low shaft inertia, to form J_r.

Number of blades B	3
Blade rotor R_t	23.5 m
Turbine rotor inertia J_r	222963 Kg.m²
Friction coefficient for the turbine b_r	743,21 N.m.s
Spring constant K_{ls}	2854 N.m/rad
Damping b_{ls}	1200 N.m.s
Gearbox ratio G	52,63
Generator inertia J_g (asynchronous machine)	12,68 Kg.m²
Friction coefficient b_g	0,2675 N.m.s

Table 1 Wind turbine characteristics

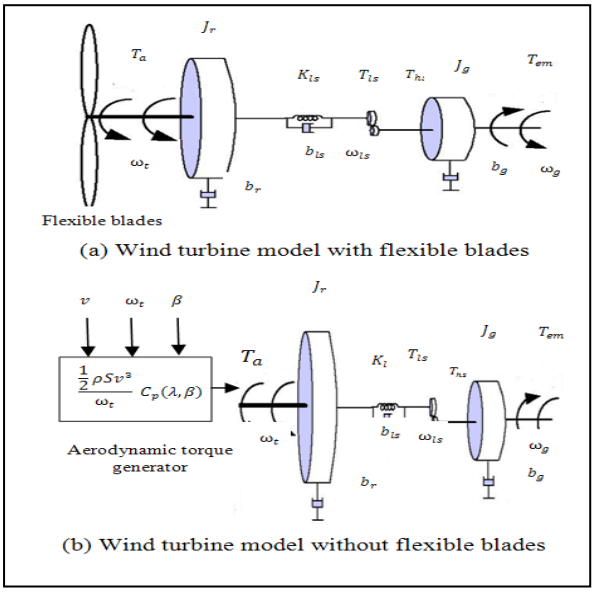

Figure 9: the two models of wind turbine

As explained in section 3, the whole aerodynamic torque is three times the aerodynamic torque obtained from the bond graph model of single blade. Figure 9(a) shows the wind turbine with flexible blade.

The second model of wind turbine is shown in Figure 9(b). In this case, hub inertia, shaft inertia and blades are lumped to form J_r, assuming that blades are rigid.

Usually, wind turbine rotor is considered as an aerodynamic torque generator. This aerodynamic torque is given by an algebraic relation (24):

$$T_a = \frac{1}{2}\rho S \frac{v^3}{\omega_t} C_p(\lambda,\beta). \qquad (24)$$

where the characteristic $C_p(\lambda,\beta)$,given in figure 10, is stored in a look up table.

Some simulations were run to verify the relevance of the generation of electromagnetic torque shown in Figure 3. In the two models, tip-speed ratio at the steady state sticks to the optimal value λ_{opt} which corresponds to the maximum power.

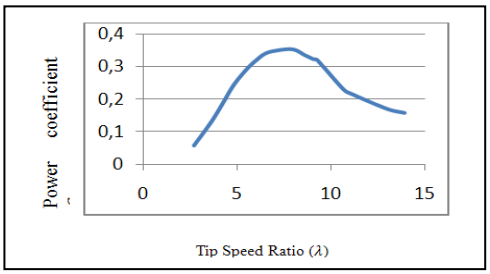

Figure 10: Typical $C_p$curve as a function of λ for $\beta = 1$ deg .

In order to compare the two models, a constant wind speed is applied (6 m/s). The relative error between the two aerodynamic torques at steady state is 0.0012 %.

Now, the wind speed increases from 6 m/s to 8 m/s as a step at t =300 s, and decreases from 8 m/s to 6 m/s at t = 350 s. The aerodynamic torque is shown in figure 11. As it can be seen, in steady state the aerodynamic torque is the same in the two models of wind turbine. However, the model of wind turbine which takes into account the flexibility of the blades, induces oscillations in the transient response.

Figure 12 and figure 13 show respectively the aerodynamic power P_{aer} and the absolute error between the aerodynamic powers of each model of wind turbine. The aerodynamic power is given by equation (25):

$$P_{aer} = T_a \omega_t. \qquad (25)$$

In steady state the absolute error is too small, however in transient state the absolute error is very important. When the wind speed increases from 6 m/s to 8 m/s, the aerodynamic power of the wind turbine model obtained from equation (25), is different for the two cases. Not taking into account the blade dynamics overestimates or underestimates the extractable power, depending on the rising or decreasing phase of the wind speed.

From figure 13,it appears that the specific case that the transient behavior here is 40s long, which involves a big amount of mechanical energy badly estimated ($\Delta E = 520Kj$) when using rigid model of the wind turbine blades.

So, neglecting blades flexibility, in transient state may induce significant error. The rigid model is too simplified to represent the whole turbine accurately, particularly in transient states.

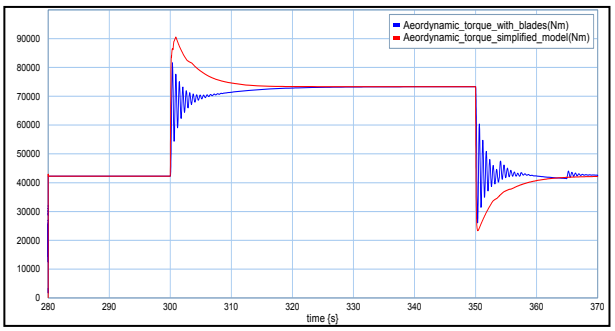

Figure 11: Aerodynamic torque

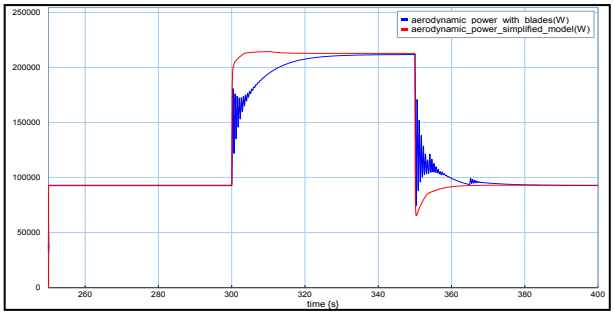

Figure 12: Aerodynamic power

Figure 14 shows the frequency spectrum for the mentioned wind velocity. This fast Fourier transform of the two aerodynamic torques shows the dominant frequency 1.7 Hz for the wind turbine model with flexible blade, which is very closed to the dominant frequency of the blades.

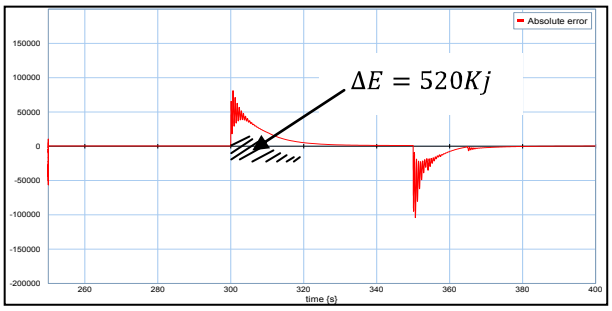

Figure 13: Absolute error between the two aerodynamic powers, ($P_{aero_{simplified}} - P_{aero_{blades}}$)

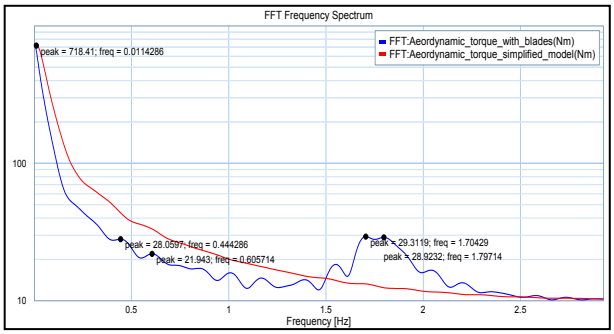

Figure 14: Frequency spectrum ($v = 6\ m/s$)

Conclusion

In this paper wind turbine models and control loop at low wind speed have been presented. Two models of wind turbine have been used. The first model is a two mass model, represented by a large inertia (turbine) and a small inertia (generator) assuming the rigidity of the blades. The second model takes into account the flexibility of blades. Aerodynamic loads are calculated using blade element momentum theory. Simulation results showed that neglecting blade flexibility may give significant error at transient sate. In steady state, wind turbine model can be expressed by the simple two-mass shaft model with reasonable accuracy.

REFERENCES

Agarwal,S.,Dauphin-Danguy,G.,Guillaud,X.,2009.Bond Graph Model of Wind Turbine Blade. Submitted to a journal.

Boukhezzar, B., Siguerdidjane ,H., 2009. Comparison Between Linear and Nonlinear Control Strategies for Variable Speed Wind Turbine Power Capture Optimization. *Proceedings of Fourth International Conference and Exhibition on Ecological Vehicles and Renewable Energies*, March 26-29, Monte-Carlo (Monaco,France).

Hansen, M.O.L., Sørensen , J.N, Voutsinas, S., Sørensen, N., Madsen, H.A., 2006. State of the art in wind turbine aerodynamics and aeroelasticity, *Progress in Aerospace Sciences*, Vol. 42, pp. 285-330.

Johnson,K.E., Fingersh,L.J., Balas,M.J., Pao,L.Y.,2004. Methods for Increasing Region 2 Power Capture on a Variable-Speed Wind Turbine. *Journal of solar energy engineering*, vol. 126**:** pp. 1092-1100.

Lanzafame, R., Messina, M., 2007. Fluid dynamics wind turbine design: Critical analysis, optimization and application of BEM theory. *Renewable Energy*, vol.32: pp. 2291- 2305.

Moriarty, P.J., Hansen, A.C.,2005, AeroDyn Theory Manual. National Renewable Energy Lab., Golden, CO (USA).

Mukherjee, A., Karmakar, Samantaray ,R., A.K., 2000. *Modelling and Simulation of Engineering Systems through Bond Graphs*. India:Narosa Publishing House.

Muyeen , S.M., Hasan Ali, Md. , Takahashi, R. ,Murata, T., Tamura, J., Tomaki , Y., Sakahara, A. , Sasano, E., 2007. Comparative study on transient stability analysis of wind turbine generator system using different drive train models. *IET Renewable Power Generation*, vol. 1: pp. 131–141.

Pao ,L.Y., Johnson ,K.E., 2009. A Tutorial on the Dynamics and Control of Wind Turbines and Wind Farms. *American Control Conference* ,pp. 2076- 2089. June 10-12, St. Louis (USA).

Pournaras, C., Riziotis,V., Kladas,A., 2008.Wind turbine control strategy enabling mechanical stress reduction based on dynamic model including blade oscillation effects. *Proceedings of the 2008 International Conference on Electrical Machines*. September 6-9, Vilamoura (Portugal).